Magnetic Susceptibility Measurement from Spatially Mapped Reaction Field

Petr Marcon, Eva Gescheidtova
Brno University of Technology, Department of Theoretical and Experimental Electrical Engineering
Brno, Czech Republic
marcon@feec.vutbr.cz
gescha@feec.vutbr.cz

Karel Bartusek
Institute of Scientific Instruments, Academy of Sciences of the Czech Republic
Brno, Czech Republic
bar@isibrno.cz

***Abstract*—This article is focused on the principles of the magnetic susceptibility measurement of the non-ferromagnetic substances using NMR tomography. Magnetic susceptibility is calculated from changes of the magnetic field close to the cylinder shaped specimen. Changes of the magnetic field in the 3D vicinity of the specimen were integrated. Before integrating of the magnetic field changes it was necessary to filter, unwrap and detect the accurate position of the specimen. Magnetic susceptibility calculated from measured data is in comparison to theoretical value, as well as model value, only slightly different.**

Keywords-NMR; magnetic susceptibility; reaction field; 3D vicinity of specimen

I. INTRODUCTION

An inhomogeneous static magnetic field (B_0 filed) generates distortion in magnetic resonance images. Measuring the spatial variation of B_0 is essential for automatic shimming. The domain source of field inhomogeneity in many MRI experiment is the variation of magnetic susceptibility of both the tissues of the human body and the implant materials.

Magnetic susceptibility provides information on the tissue relative iron concentration that is useful for diagnosis and treatment of a number of diseases such as sickle cell disease, aplastic anaemia, thalassemia, haemochromatosis and Parkinson´s disease. In magnetic resonance imaging, the susceptibility effects have Essentials relevance for imaging contrast and artifact correction, functional brain imaging, molecular imaging and the measurement of blood oxygenation. Thus, it is highly significant to develop methods that can measure arbitratry susceptibility distributions.

The knowledge of the magnetic susceptibility of tissues or various implants can help us to minimize the effect of magnetic susceptibility in MRI images via modification of pulse sequences, i.e. to correct artifacts in MRI images. These artifacts are manifested by the loss of signal, and new artifacts appear in the vicinity. For example, functional brain imaging using the gradient-echo planar imaging is based on blood oxygenation level-dependent (BOLD) susceptibility effects, which are believed to be dependent on neuronal activity in specific regions of the brain, as a result of cognitive tasks of human subjects (as well as animals) [1, 2]. Depending on the location of the cortical areas that are involved in an fMRI study, the BOLD effect is strongly influenced by local field inhomogeneities created by differences in magnetic susceptibility – between air and tissue for example, and results in severe image distortion and signal loss. Signal loss is a major problem in fMRI studies [3, 4]. The measurement of magnetic susceptibility of magnetically compatible materials (the NMR measuring method enables obtaining a signal even inside the specimen) has been the subject of study undertaken by Lin, who calculates susceptibility using a delineated area inside the specimen [5, 6].

In this paper, we deal with magnetic susceptibility measurement of non ferromagnetic materials in macroscopic view. For calculating of magnetic susceptibility we used 3D (three dimensional) mapped reaction filed in the vicinity of specimen. Chapter II and III the basis of method of magnetic susceptibility measurement is described. Our experimental measurements and signal processing are mentioned in chapter IV. The conclusions and discussions about our results are presented in chapter V.

II. METHODS

This method of susceptibility measurement is based on the assumption of constant magnetic flux in the working space of superconducting magnet. Inserting a specimen with magnetic susceptibility χ_s causes local deformation of previously homogeneous magnetic field – for illustration see Fig. 1.

The magnitude of these deformations depends on the difference of magnetic susceptibility of the specimen χ_s and of its vicinity χ_v, on the volume and shape of the specimen, and on the magnitude of basic field B_0.

 ISBN: 978-1-61208-184-7

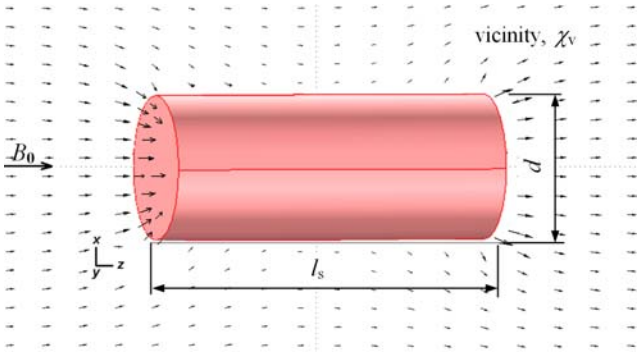

Figure 1. Magnetic flux density field deformation due to paramagnetic specimen.

III. THEORETICAL ANALYSIS

The method was verified via an experiment with a number of specimens on a 4.7 T/76 mm MR tomograph in ISI AS Brno (^{1}H ≈ 200 MHz). The specimens to be measured were of different materials in the shape of cylinders 3 mm in diameter and 10 mm in length (No. 2 in Fig. 2). They were placed in a glass container in the shape of a 40 x 40 x 40 mm cube (No. 1 in Fig. 2) filled with a solution of water with this concentration: 1 liter deionized water, 1.2 gram $NiSO_4$ and 2.6 gram NaCl in order to shorten the relaxation times to $T_1 = T_2 = 130$ ms. Magnetic susceptibility of this solution was $\chi_v = -13.0 \cdot 10^{-6}$. When measuring materials with nearly the same susceptibility, the reaction field will not be induced.

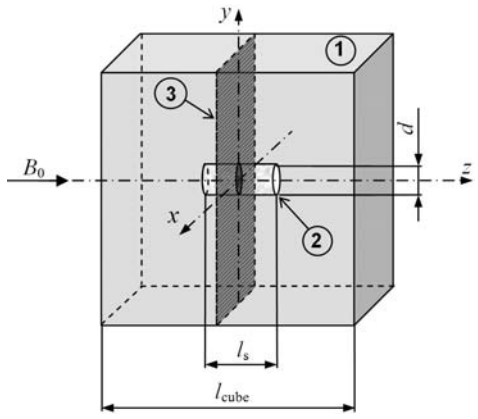

Figure 2. Configuration of system – vicinity with specimen.

One of the MR measurement methods – the Gradient echo (GE) method is very sensitive to inhomogeneities of the static magnetic field and this can be useful for susceptibility measurement [5]. Because the reaction field is generated proportionally to material susceptibility, it is possible to use the GE method for its measurement. The GE sequence depicted in Fig. 3 with the parameters: echo time T_E =17 ms, repetition time T_R = 5 s, was used to obtain an MR image of the reaction field in the vicinity of the measured specimen.

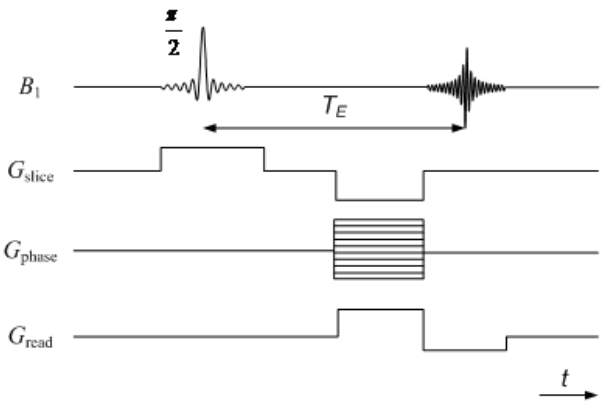

Figure 3. Diagram of the Gradient echo measurement sequence used.

The MR image obtained using the GE technique is phase-modulated by the magnetic induction change and, on condition of proper experiment arrangement we can obtain the image of magnetic field distribution in the specimen vicinity. For the calculation of the reaction field ΔB we can give the following relation:

$$\Delta B = B - B_0, \tag{1}$$

which is the material's own field caused by magnetization. Transversal magnetization $M_\perp$ is for the GE method described by the equation:

$$M_\perp(T_E) = M_0(T_E)\, e^{-\frac{T_E}{T_2^*}} e^{-j\gamma \Delta B T_E}, \tag{2}$$

where M_0 is the transversal magnetization obtained immediately after excitation, which has been exponentially decreased in time by e^{-T_E/T_2^*}. Here T_2^* is effective relaxation time. The term $e^{-j\gamma \Delta B T_E}$ describes the phase modulation of magnetization, induced by reaction field ΔB. It is evident that the phase part of complex image can be used to obtain the spatial distribution of reaction magnetic field flux density ΔB (see [7, 8]):

$$\Delta B = \frac{\Delta \varphi}{\gamma \cdot T_E}, \tag{3}$$

where γ is the gyromagnetic ratio of reference substance, $\Delta\varphi$ is the phase image, and T_E is the echo time of the GE measuring sequence. From (2) we can see two opposite requirements for the echo time: with longer time T_E we have a magnetization which is more sensitive to the reaction field, but due to relaxation time T_2^* we also have a lower signal-to-noise ratio.

 ISBN: 978-1-61208-184-7

IV. EXPERIMENTS AND RESULTS

From magnetic resonance system we obtain two dimensional data (image matrix 128 x 128 px). An example of 1 slice you can see in Fig. 2 point 3. The measurement was made for 64 slices. These data were further processed in the Marevisi and Matlab programs. To remove the effect of the inhomogeneities of magnetic field background we used two measurements – with embedded specimen and blind measurement (without specimen). The procedure of processing data from the two measurements is indicated in Fig. 4. Both data matrices were transformed using FFT in the Marevisi program. Marevisi is a program for data processing and visualization for MRI [9]. The program was developed by Jana and Zenon Starcuk and Piotr Kozlowski. Further processing continues in the Matlab program, using the algorithm created. From the complex 3D data points, only the phase component was further used. Because the phase image was periodically wrapped (this means discontinuities in the phase change between $-\pi$ and π), the next operation was unwrapping. To map the reaction field, measuring with the GE pulse sequence for two echo times T_E can be employed [10,11]. The blind phase image was subsequently subtracted from the one with specimen to eliminate the inhomogeneity of the basic tomograph field. The differential phase image was converted to the reaction field magnetic flux density using (3). Inside the specimen are any hydrogen atoms. Therefore we obtain any inside the specimen any useful signal, but only noise. For calculation of magnetic susceptibility we use only vicinity of the specimen and we replace the measured data inside in specimen with zeros.

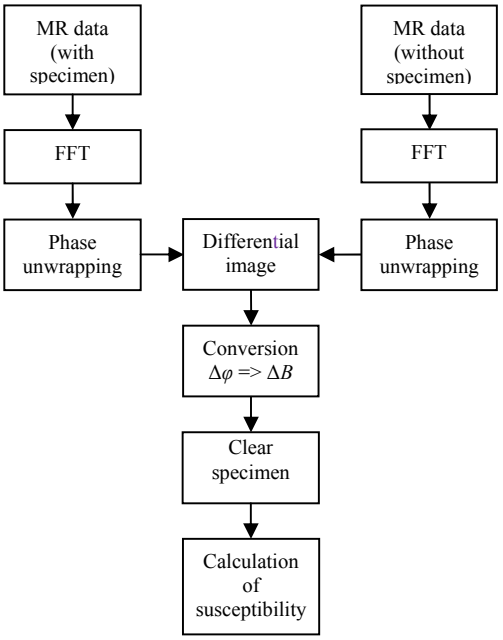

Figure 4. Diagram of image processing of obtained MR GE phase images. Input data are two complex matrices (MR image with and without specimen).

Fig. 5 is the graphical representation of the distribution of reaction magnetic field ΔB in a section through the aluminum specimen measured (the section corresponds to point 3 in Fig. 2). The picture was created in Matlab program from the measured values of reaction field in the vicinity of measured specimen. In the picture you can see the zeros place, there was measurement. Magnetic susceptibility was calculated from 3D distribution of the reaction magnetic field by relation (4).

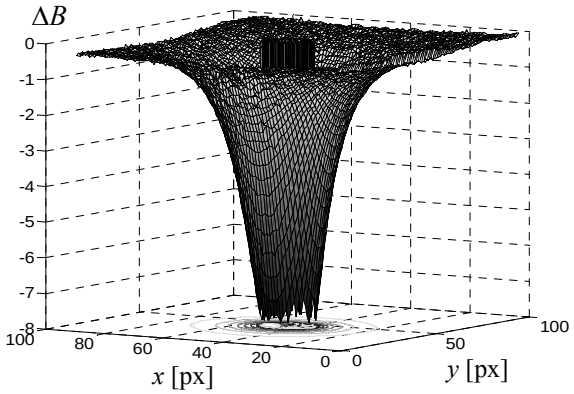

Figure 5. Distribution of reaction magnetic field ΔB in a section through plane x,y in the centre of aluminium cylinder measured.

The last step is susceptibility calculation. For discrete processing of the data measured will lead to equation (4). This equation will be used to calculate differential magnetic susceptibility χ_Δ. To obtain magnetic susceptibility of the specimen χ_s we substitute the value χ_Δ into equation (5).

$$\chi_\Delta = \frac{1}{M \cdot N \cdot P} \sum_{x=1}^{M} \sum_{y=1}^{N} \sum_{z=1}^{P} \Delta B_{xyz} = \frac{1}{|V_s|} \sum_{V_s} \Delta B \,, \qquad (4)$$

where V_s is the volume of the measured specimen in the 3D image.

By relation (5), magnetic susceptibility of the specimen χ_Δ can be calculated from the differential value of magnetic susceptibility:).

$$\chi_s = -\frac{2\chi_\Delta + \chi_v(\chi_\Delta + 1)}{\chi_\Delta - 1}, \qquad (5)$$

where χ_v is magnetic susceptibility of water in the cylinder vicinity.

The results of our measurement you can see in the Table I. There, the known values of susceptibility are denoted χ_k and the values obtained by measuring and data processing are denoted χ_m.

 ISBN: 978-1-61208-184-7

TABLE I. RESULTS OF MAGNETIC SUSCEPTIBILITY OF SPECIMEN

Material	Purity [%]	Shape	Size [mm]	χ_k [$\times 10^{-6}$]	χ_m [$\times 10^{-6}$]
Al	99.50	Cylindrical bar	d=4.00; l_s=10.00	22.00	22.71
Cu	99.91	Cylindrical bar	d=2.70; l_s=10.05	-9.60	-9.72

V. CONCLUSION

The calculation of magnetic susceptibility by relations (4) and (5) was verified experimentally on an MR tomography system and via processing the data measured as shown in Fig. 4. The specimens were a copper and an aluminium cylinder, of known magnetic susceptibility and purity (see Table I). In comparison with the known magnetic susceptibility values the measuring error is in both cases less than 3.23 %. However, there are some limitations to the proposed method. A disadvantage of the proposed method consists in that the accuracy of magnetic susceptibility calculation depends on the shape of specimen (have to be cylinder or block). In the future, the measuring method can be used to establish the susceptibility of tissues or implants in the human body and, thanks to this knowledge; it will be possible to attenuate the artifacts in MRI images produced by these materials.

ACKNOWLEDGMENT

This work supported within GA102/1/0318 and CZ.1.05/2.1.00/01.0017 (ED0017/01/01) and FEKT-S-11-5/1012.

REFERENCES

[1] S. Ogawa, T. M. Lee, A. S. Nayak and P. Glynn, "Oxygenation-sensitive contrast in magnetic resonance imaging of rodent brain at high magnetic fields," Magnetic Resonance in Medicine, vol. 14,1990, pp. 68-78, 1990.

[2] R. Deichmann, O. Josepshs, D. Hutton, D. R. Corfiled and R. Turner, "Compensation of susceptibility- induced BOLD sensitivity losses in echo-planar fMRI imaging," Neuroimage, vol. 15, pp. 120-135.

[3] J. Y. Chung, H. W. Yoon, Y. B. Kim, H. W. Park and Z. H. Cho, "Susceptibility compensated fMRI study using a tailored RF echo-planar imaging sequence," Journal of Magnetic Resonance Imaging, vol. 29, 2009, pp. 221-228.

[4] L. Li, "Magnetic susceptibility quantification for arbitrarily shaped objects in inhomogeneous fields," Magnetic Resonance in Medicine, vol. 46, 2001, pp. 907-916.

[5] P. Marcon, K. Bartusek, M. Burdkova and Z. Dokoupil, "Magnetic Susceptibility measurement using 2D magnetic resonance imaging," Measurement Science and Technology, vol. 22, 2011, doi:10.1088/0957-0233/22/10/10570.

[6] K. Bartusek, Z. Dokoupil, E. Gescheidtova, "Magnetic field mapping around metal implants using an asymmetric spin-echo MRI sequence," Measurement Science and technology, vol. 17, 2006, pp. 3293-3300.

[7] M. Steinbauer and K. Bartusek, "Magnetic susceptibility measurement using magnetic resonance tomograph," Acta Technica CSAV, vol. 53, 2008, pp. 45-63.

[8] M. Vlaardingerbroek, "Magnetic Resonance imaging," Springer Verlag, 2000.

[9] K. Bartusek, E. Kadlecova, P. Fiala and J. Mikulka, "Magnetic field deformation numerical modelling in relation to measured susceptibility using MR system," Radioengineering, vol. 17, 2008, pp. 249-266.

[10] B. Guru and H. Hiziroğlu, "Electromagnetic field theory fundamentals," Cambrigdge University Press, 2004.

[11] K. Bartusek, Z. Dokoupil and E. Gescheidtova, "Mapping of magnetic field around small coils using the magnetic resonance method, Measurement Science and Technology, vol. 18, 2007, pp. 2223-2230.

[12] P. Andris and I Frollo, "Optimized measurement of magnetic field maps using NMR", Measurement Science and Technology, vol. 22. 2011.

 ISBN: 978-1-61208-184-7